DOI https: //doi. org/10.1007/s11595-025-3061-4

Fatigue Strength Analysis of Dissimilar Aluminum Alloy TIG Welds

LIAO Xiangyun[1], WANG Ruijie[1*], LIU Guoshou[2], ZHAO Pinglin[1]

(1. Faculty of Mechanical and Electrical Engineering, Kunming University of Science and Technology, Kunming 650500, China; 2. Faculty of Civil Engineering and Mechanics, Kunming University of Science and Technology, Kunming 650500, China)

Abstract: The constant amplitude loading fatigue tests were carried out on the 6061/7075 aluminum alloy TIG fillet welded lap specimens in this study, and the weld seam cross-section hardness was measured. The experimental results show that most specimens mainly failed at the 7075 side weld toes even though the base material tensile strength of 7075 is higher than that of 6061. The maximum stress-strain concentration in the two finite element models is located at the 7075 side weld toe, which is basically consistent with the actual fracture location. The weld zone on the 7075 side experiences severe material softening, with a large gradient. However, the Vickers hardness value on the 6061 side negligibly changes and fluctuates around 70 HV. No obvious defects are found on the fatigue fracture, but a large number of secondary cracks appear. Cracks germinate from the weld toe and propagate in the direction of the plate thickness. Weld reinforcement has a serious impact on fatigue life. Fatigue life will decrease exponentially as the weld reinforcement increases under low stress. It is found that the notch stress method can give a better fatigue life prediction for TIG weldments, and the errors of the predicted results are within the range of two factors, while the prediction accuracy decreases under low stress. The equivalent structural stress method can also be used for fatigue life prediction of TIG weldments, but the errors of prediction results are within the range of three factors, and the accuracy decreases under high stress.

Key words: TIG welding; notch stress method; equivalent structural stress method; fatigue life; finite element analysis

1 Introduction

Aluminum alloy is one of the most widely used materials in aerospace, with light-weight and high-strength as its biggest characteristics. It is used in key plane parts such as skin and forged rings[1]. However, one single material would not meet the actual engineering requirements in many cases, and the connection between different alloys tends to combine the advantages of different materials to reduce product costs[2]. Welding is also a convenient way to connect dissimilar aluminum alloys and other metals among other common connection methods in addition to mechanical connection[3].

The welding of aluminum alloy using Tungsten inert gas (TIG) is a widely employed technique. Its stable working current makes it more suitable for aluminum alloy sheets. AC TIG welding can also play a significant role in refining grain size and improving weld strength[4]. TIG welding is the most common process in 6061 aluminum alloy welding[5], but it is quite difficult to weld 7075 by this method because it is easy to produce cracks and porosity defects that affect the fatigue strength[6]. This method is also accompanied by residual stresses. The incomplete fusion defects will increase the risk of specimen fracture in special fields such as aerospace and have a high potential safety hazard. Fatigue failure tends to occur in load-bearing parts[7]. Therefore, many researchers have done a lot of research on the performance of welds.

Ren[8] carried out a high-cycle fatigue failure analysis on TA15 titanium alloy TIG butt weld specimens and found that the specimens in the fatigue tests mainly broke at the junction of the heat-affected zone and the base metal zone, rather than at the weld toe. This was due to the mismatch of high grain boundaries between the two regions, and the accumulation of dislocation

(Received: Aug. 25, 2023; Accepted: Nov. 21, 2024)

LIAO Xiangyun(廖祥雲): MPhil candidate; E-mail: 1215433850@qq.com

*Corresponding author: WANG Ruijie(王瑞杰): Ph D; E-mail: wrj@kust.edu.cn

Partially funded by the National Natural Science Foundation of China (No.51065012)

phenomenon produces a stress concentration. Wan[9] used swing TIG welding to weld 2219-T8 aluminum alloy. It was found that the weld shape would affect the stress concentration at the weld toe. Thus, the tensile properties of the joint were affected, but the influences on the microstructure and microhardness were small. Kumar[5] discussed the effect of welding speed on the microstructure and mechanical properties of the 6061 aluminum alloy TIG butt weld zone and found that the welding speed would affect the grain size and tensile strength of the fusion zone, which may be caused by the change of heat input. Zhao[10] found that the corrosive medium would seriously reduce the high cycle fatigue life of 6005/5083 aluminum alloy TIG welding and the fracture locations will be different. The increase of acid concentration would affect the crack formation mechanism.

Accurately evaluating the fatigue life of welds is a key point in engineering. The recommended standards of IIW (International Institute of Welding, IIW) proposed some methods for predicting the fatigue life of notched parts, such as the notch stress method and the hot spot stress method. However, weld defects and surface parameters can affect fatigue life. Some researchers[11,12] have proposed many fatigue life prediction models based on loading conditions and microstructure parameters, which are more practical and have higher accuracy. But their applicability has decreased, while welding defects under fatigue loads can reduce the effective load-bearing area of welded joints and generate stress concentration. There is an urgent need to evaluate the fatigue properties of this kind of welds as load-bearing parts in practical applications.

The constant amplitude loading fatigue tests and weld seam cross-section hardness tests are carried out on the overlap specimens of TIG fillet welded 6061/7075 aluminum alloy, which were welded with ER5356 alloy wire as filler in this paper. The fatigue properties and failure modes were analyzed, and the softening of the weld zone was observed. The fatigue lives were predicted by finite element stress-strain analysis combined with both the notch stress method and equivalent structural stress method, and then compared with the experimental fatigue lives.

2 Experimental

The experimental materials are 7075 and 6061 aluminum alloy sheets with a thickness of 3 mm. The chemical compositions of the materials are shown in Table 1. The TIG fillet welded lap joint specimens were welded after polishing the surface of the base metals, and ER5356 welding wire was used as filler for welding. The welded plates were then cut into specimens with dimensions as shown in Fig.1. Two equal-thickness spacers were placed at the clamped ends to prevent the generation of bending moments in fatigue testing and static tensile testing. The tensile strength of the specimen was 188 MPa, measured by the universal material testing machine produced by the Suns®. The constant amplitude fatigue tests were carried out for the specimens on the MTS809 fatigue testing machine with a ramp loading waveform at a frequency of 10 Hz. Kept the average load constant and changed the magnitude of the load amplitude during the experiments. The number of cycles at fracture for each load amplitude was recorded as experimental life. And the fracture surface of the specimen after fatigue testing was well preserved, as the fracture surface would oxidize in air. It was important to observe the fatigue fracture mode of the tested specimens and make good records of fracture locations.

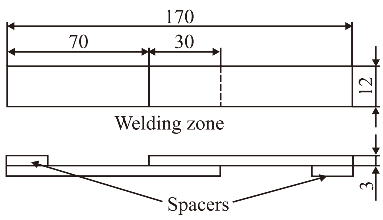

Fig.1 6061/7075 aluminum alloy welding specimens

3 Analysis of test results

3.1 Fatigue tests

The fatigue test results are shown in Table 2. Most of the fracture positions are located on the 7075 side,

Table 1 Chemical compositions of base metal and welding wire/wt%

Material	Zn	Mg	Cu	Si	Cr	Fe	Mn	Ti	Al
7075	5.1-6.1	2.1-2.9	1.2-2.0	⩽0.4	0.18-0.28	⩽0.5	⩽0.3	⩽0.2	Bal.
6061	0.25	0.8-1.2	0.15-0.4	0.4-0.8	0.04-0.35	0.7	0.15	0.15	Bal.
ER5356	⩽0.1	4.5-5.5	⩽0.1	⩽0.25	0.05-0.2	⩽0.4	0.05-0.2	0.06-0.2	Bal.

Table 2 Results of fatigue tests

Number	Maximum load/MPa	Minimum load/MPa	Life/Cycle	Fracture position
W01	169.444	13.889	4 037	7075 side weld toe
W08	158.333	25	9 951	7075 side weld toe
W03	152.778	30.556	6 676(Simultaneous fracture)	7075 side weld seam 6061 side weld seam
W05	147.222	36.111	14 881	7075 side weld toe
W06	141.667	41.667	14 743	7075 side weld toe
W07	136.111	47.222	14 504(Simultaneous fracture)	7075 side weld seam 6061 side weld seam
W09	163.889	19.444	8 099	7075 side weld toe
W10	130.556	52.778	59 627	7075 side weld toe
W12	133.333	50	21 521	7075 side weld toe
Y01	125	58.333	79 611	7075 side weld toe
Y02	138.889	44.444	29 143	7075 side weld toe
Y03	119.444	63.889	145 616	7075 side weld toe
Y04	172.222	11.111	6 150	7075 side weld toe
Y05	175	8.333	7 144(break firstly) 7 144	7075 side weld toe 6061 side weld seam
Y06	180.556	2.778	442(break firstly) 506	6061 side weld seam 7075 side weld toe
Y07	177.778	5.556	3 449	7075 side weld toe
Y08	179.167	4.167	3 818	7075 side weld toe
Y09	122.222	61.111	137 043	7075 side weld toe
Y11	150	33.333	9 233	7075 side weld toe
Y13	127.778	55.556	36 482	7075 side weld toe

(Tips: The W-series specimen is from the same weldment, and the Y-series specimen is from another weldment in the table. The two types of specimens adopt the same welding process and the welds are the same. Simultaneous fracture means that when the specimen as shown in Figs.2(a) and 2(b) breaks, two brittle sounds are heard instantaneously, which makes it difficult to distinguish the fracture sequence)

and the cracks originate from the weld toe and propagate along the plate thickness. The fracture is almost linear. Both 6061 and 7075 sides of specimen W07 fracture at the weld seam, and the crack gradually propagates along the normal direction of the weld seam, with serious distortion occurring during the fracture. The 7075 side weld toe of specimen Y05 fractures first, while the 6061 side weld of specimen Y06 fractures first. Although the sequence of the fracture of specimens Y05 and Y06 is different, 7075 sides are broken at the toe of the weld, and 6061 sides are all broken at the weld seam. The fracture mode of specimen Y13 is seen in most specimens. Three fracture modes are shown in Fig.2. The weld toes of all specimens are fatigue damaged, but there is no separate fracture on 6061 side.

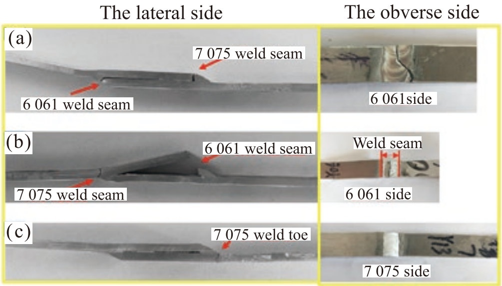

Fig.2 Fracture position of the specimens: (a) specimen W07; (b) specimen Y06; (c) specimen Y13

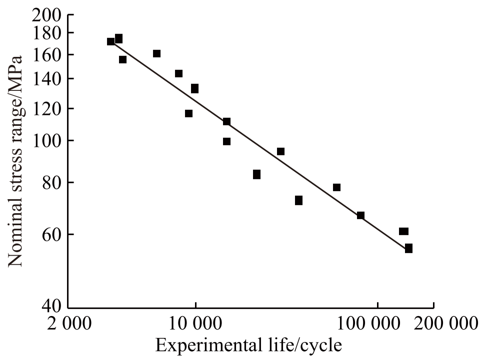

Fig.3 *S-N* curve of 7075-side fracture specimens

The experimental load-life relationship curve (*S-N* curve) of 7075 side fracture specimens is fitted under the double logarithmic coordinates. The fitting results are shown in Fig.3.

Here, the nominal stress is the load range divided by the cross-sectional area of the plate. It can be seen from Fig.3 that there is a good linear relationship between nominal stress and fatigue life. The *S*-*N* curve relationship is shown in Eq.(1).

$$\lg S_0 = -0.303 \cdot \lg N_0 + 3.306 \quad (1)$$

where S_0 is the nominal stress range, N_0 is the experimental life.

3.2 Hardness tests

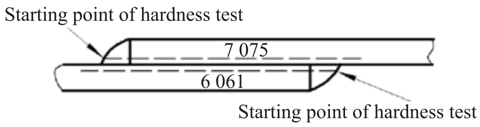

Fig.4 Dotting position

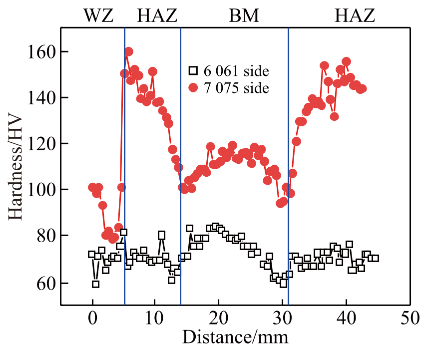

Fig.5 Hardness distribution

HMV-G-FA full-automatic Vickers microhardness tester was used for weld seam cross-section hardness measurements. A load of 200 g was applied and a testing point was made at interval of 0.5 mm during the test. The testing points positions are shown in Fig.4. The testing holding period was 10 s. The test results are shown in Fig.5. The hardness test points cover the weld zone (WZ), heat affected zone (HAZ) and base metal zone (BM). On the whole, the hardness values of 6061 sides and 7075 sides are quite different, but the hardness values in the weld zone are relatively close to each other. The hardness of 7075 sides fluctuates more greatly. The average hardness value of the weld zone on this side is the lowest, at approximately 90 HV, while the hardness of the heat-affected zone is the highest, which shows a downward trend with the increase of the distance from the weld zone. The hardness distribution in the base metal zone is relatively stable, at about 110 HV. The hardness values of each area on 6061 sides are similar, and the hardness values in weld zone and in heat affected zone are almost the same. But the hardness value of base metal on this side is the highest. The overall hardness fluctuates around 70 HV. The softening phenomenon of weld zone on 7075 sides is serious, but not on 6061 sides.

3.3 Fatigue fracture analysis

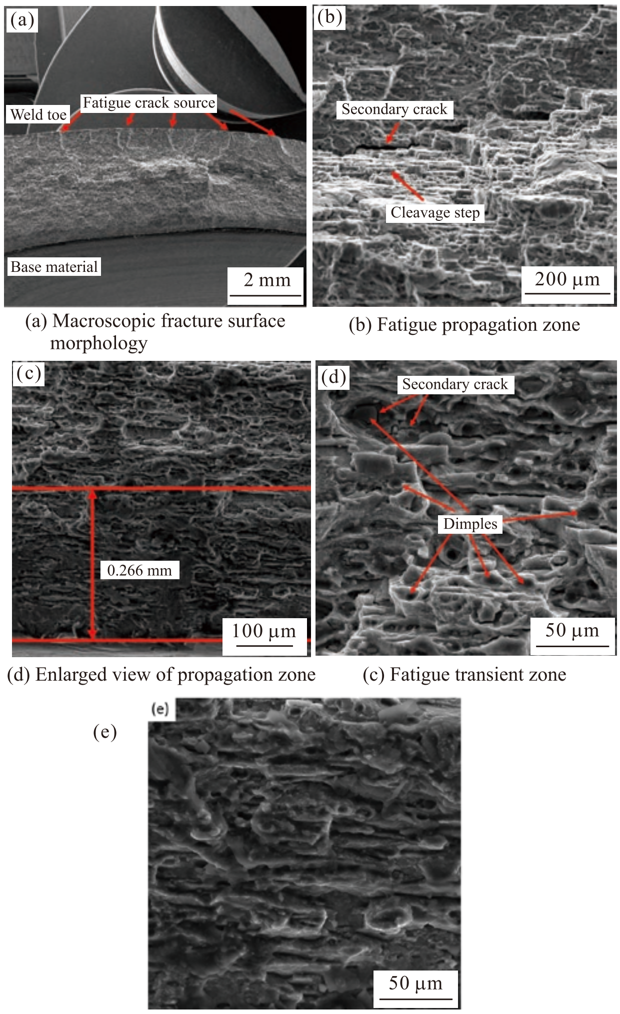

(a) Macroscopic fracture surface morphology (b) Fatigue propagation zone

(d) Enlarged view of propagation zone (c) Fatigue transient zone

(e) Enlarged view of transient zone

Fig.6 Fatigue fracture morphology of specimen Y02

The fracture position of specimen Y02 is at the weld toe on 7075 side. It can be seen from Fig.6(a) that there are multiple crack sources at the weld toe. Cracks initiate from the surface of the weld toe and then propagate along the thickness direction, leading to the final fracture of the specimen. A long secondary crack and cleavage step are observed in the center of the fatigue propagation zone (Fig.6(b)). There is a significant stress concentration at the cleavage step, which accelerates crack propagation and affects fatigue life, leading to the generation of secondary cracks here. It is found that there are many small secondary cracks on the surface of the propagation zone, accompanied by a small number of dimples (Fig.6(d)). The fracture surface of the instantaneous fracture zone is relatively flat, presenting a planar fracture (Fig.6(c) and Fig.6(e)). These dimples are formed by plastic deformation under fatigue load due to uneven distribution of grain size in the weld seam. Dimples become areas of stress concentration during fatigue loading, resulting in small secondary cracks appearing at the bottom of some dimples.

4 Finite element analysis and fatigue life prediction

4.1 Fatigue life prediction based on notch stress method

4.1.1 Establishment of finite element model

It is difficult to obtain the stress state based on the analytical solution due to the sharp notch near the weld, which results in high stress concentration. The notch stress method is based on the linear elastic assumption. The sharp notch near the weld is equivalent to a virtual circle, and the stress at the notch at the weld toe is used as the fatigue evaluation parameter[13]. The notch stress can be well evaluated by using finite element analysis software.

The specimens were modeled according to the real size, and the stress concentration was at the arc transition. IIW recommends that when the thickness of the specimens is less than 5 mm, the reference arc radius should be 0.05 mm. And the number of elements around the arc cannot be less than 40[14]. The number of grids can be increased appropriately to reduce the error when meshing the stress concentration at the weld toe. CPE4 plane strain element was used in order to simplify the specimen loading condition for stress calculation. The whole model had 22 759 nodes and 22 004 elements. The left end (6061 side) of the specimen was fully constrained, and for the right end (7075 side) of the specimen only the displacement in the longitude direction was not constrained, which was left for loading application. The finite element model established is shown in Fig.7.

The two materials were assigned to the BM and WZ respectively. It was assumed that the material properties of each part were uniform and the influence of small deformation of the specimen was ignored during the analysis. The notch stress method only requires linear elastic finite element analysis. The material properties of 7075, 6061, and ER5356 are shown in Table 3. In order to simplify the model, it was assumed that the material in each zone of the specimen was uniform and ignored the influence of the material shift in the HAZ. ER5356 welding wire was applied to the fillet weld, and 7075 and 6061 material properties were applied to the BMs respectively (as shown in Fig.8).

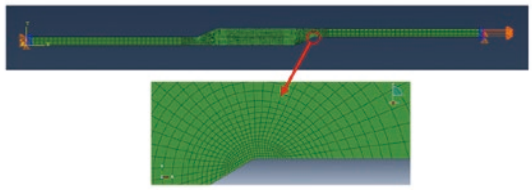

Fig.7 Mesh division under notch stress method

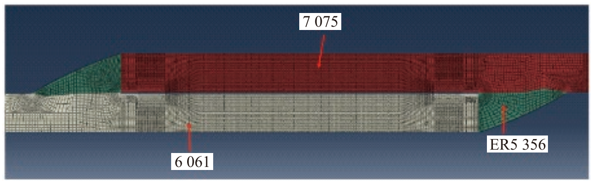

Fig.8 Material assignment of model

Table 3 Material properties

Materials	Elastic modulus /MPa	Poisson's ratio
7075	72 800	0.33
6061	67 800	0.33
ER5356	71 400	0.31

4.1.2 Fatigue life prediction

The S-N curve of the welded joint defined by IIW is shown in Eq.(2)[15]:

$$\left.\begin{cases} N = 2\times10^{6}\times(\Delta\sigma / FAT)^{-k}, N \le N_{\mathrm{K}} \\ N = (2\times10^{6}\times FAT^{K} / N_{\mathrm{K}})^{k^{*}/k}(N_{\mathrm{K}} / \Delta\sigma^{k^{*}}), N > N_{\mathrm{K}} \end{cases}\right\} \tag{2}$$

where N is the predicted life, $\Delta\sigma$ is the stress variation range, FAT is the fatigue grade value, k is the slope of the upper half of the S-N curve, k^{*} is the slope of the lower half of the S-N curve, N_{k} is the curve inflection point.)

It is generally believed that the fatigue life N of aluminum alloy exceeds 10^{7}, and it will enter the high cycle fatigue stage. N_{k} is taken as 10^{7}. Literature[16] gives FAT values of aluminum under different virtual radii, as shown in Table 4.

Here Von Mises stress is used for fatigue life prediction according to IIW recommendation. Fig.9 is the finite element Von Mises stress nephogram obtained from the analysis of the specimen with the maximum load of 163.889 MPa. It can be seen that the maximum stress node is at the 7075 side weld toe, which is consistent with the actual fracture position of the specimen. Select the Von Mises stress maximum element, output

Table 4 FAT value under different reference radius and strength assumptions

Reference radius of notch circle	1	1	0.05	0.05
Strength assumption	PSH	Von Mises	PSH	Von Mises
Aluminium	71	63	178	158

the stress variation range and then supersede it into Eq.(2) to calculate the predicted life.

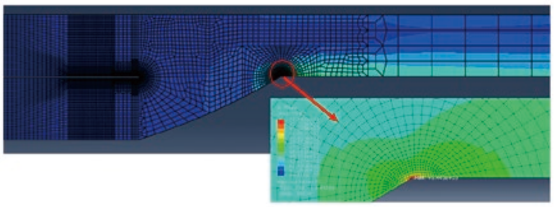

Fig.9 Von Mises stress nephogram of W09 specimen

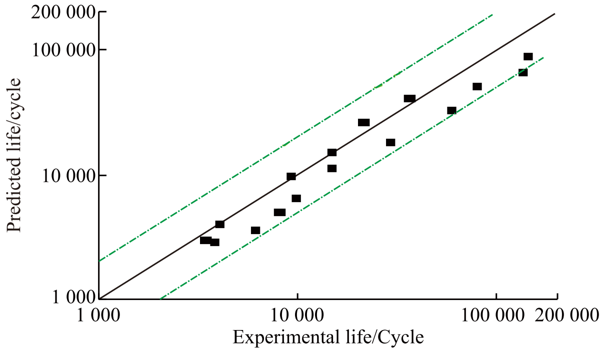

Fig.10 Life prediction results of notch stress method

The results of fatigue life prediction based on the notch stress method are shown in Fig.10. The errors of the predicted life are almost all within 2 factors. It can be seen from Fig.10 that the predicted lives are slightly shorter than the experimental lives, and all are located around the centerline. The predicted results tend to be conservative, relatively lower and close to the lower two-factor line, and the prediction accuracy gradually decreases as the load decreases.

4.2 Analysis of the influence of weld reinforcement on fatigue life based on the notch stress method

There is a slight difference in weld reinforcement shapes after TIG welding specimens were filled with welding wires. Due to it being difficult to measure the reinforcement, its impact on fatigue life was overlooked in previous fatigue life analysis. In order to investigate the effect of weld reinforcement on fatigue life, it was assumed that all models in this section had the same effective bearing length and lap length. Set the weld reinforcement as a unique variable in finite element stress analysis. However, due to the fact that all the welds of the specimens were protruding outwards, only a model with a weld reinforcement of 0-0.75 mm was established here (Fig.11 and Fig.12).

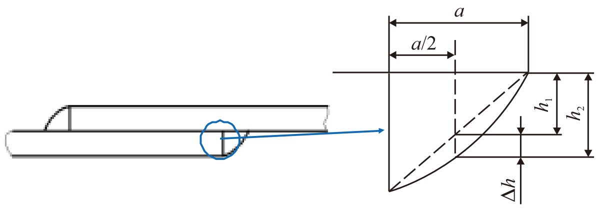

Fig.11 Schematic diagram of weld reinforcement

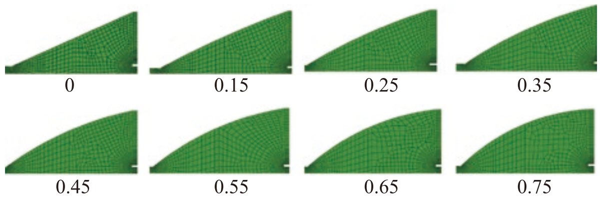

Fig.12 Finite element model of different weld reinforcement

where, Δh represents the weld reinforcement; h_2 is the height of the complete weld seam; h_1 is the height of the weld seam without reinforcement; a is the effective bearing length.

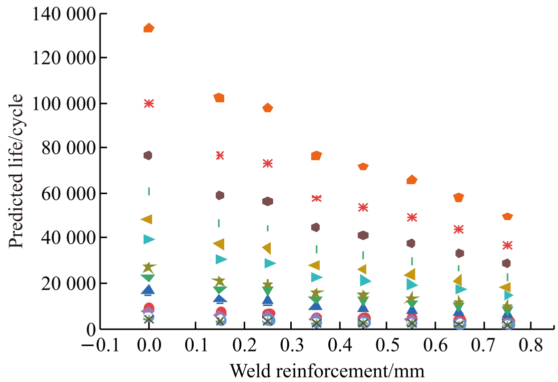

Fig.13 Relationship diagram between weld reinforcement and predicted life

In order to accurately measure its impact on fatigue life, the notch stress method is once again used for fatigue life assessment. From Fig.13, it can be observed that under high stress conditions, the effect of weld reinforcement on fatigue life is relatively small, and there is almost no change in predicted lives that fall into a straight line. The weld reinforcement has a significant impact on fatigue life under low stress conditions. When the change in weld reinforcement is within 0.75 mm, the service life has increased almost by three times.

4.3 Fatigue life prediction based on equivalent structural stress method

4.3.1 Numerical solution of equivalent structural stress

The equivalent structural stress method is based on structural mechanics and fracture mechanics. It overcomes the shortcoming of finite element analysis that is sensitive to mesh and directly describes the influence of welding joint form, load, boundary conditions, size effect, and other factors. A main *S-N* curve can be used to analyze the fatigue strength at the weld toe, which covers the effect of welding residual stress and welding method.

It is necessary to calculate the structural stress before calculating the equivalent structural stress. This kind of stress is caused by the stress concentration at the welding position and the stress distribution is relatively nonlinear. Zhang[17] divided this highly nonlinear force into two parts. The first part is the force balanced with the external force, also known as structural stress. The second part is the residual stress after removing the first part, also known as notch stress. The value of structural stress is the sum of membrane stress and bending stress:

$$\sigma_{\mathrm{s}}=\sigma_{\mathrm{m}}+\sigma_{\mathrm{b}} \tag{3}$$

Membrane stress:

$$\sigma_{\mathrm{m}}=\frac{1}{t}\int_{-t/2}^{t/2}\sigma_x(y)\mathrm{d}y=\frac{f_y}{t} \tag{4}$$

Bending stress:

$$\sigma_{\mathrm{b}}=\frac{6}{t^2}\int_{-t/2}^{t/2}y\sigma_x(y)\mathrm{d}y=\frac{3m_x}{t^2} \tag{5}$$

where f_y is a linear force at the weld toe; m_x is a linear moment; t is the plate thickness of the specimen.

The remaining life of the joint depends on the crack propagation life once the fatigue crack occurs in the welded part. The number of failure cycles of welded joints can be estimated based on the principle of fracture mechanics. The crack growth at the weld can be divided into short crack expansion and long crack expansion through the analysis of a large number of fatigue test data[18]. The Paris formula is redefined on this basis:

$$\frac{\mathrm{d}a}{\mathrm{d}N}=CM_{kn}^{n}(\Delta K)^m \tag{6}$$

$$\Delta K=\sqrt{t}[\Delta\sigma_{\mathrm{m}}f_{\mathrm{m}}(a/t)+\Delta\sigma_{\mathrm{b}}f_{\mathrm{b}}(a/t)] \tag{7}$$

By integrating Eq.(6) and Eq.(7):

$$N=\int_{a/t\to 0}^{a/t=1}\frac{t\mathrm{d}(a/t)}{C(M_{\mathrm{kn}})^n(\Delta K)}=\frac{1}{C}t^{1-\frac{m}{2}}(\Delta\sigma_{\mathrm{s}})^{-m}I(r) \tag{8}$$

$$f_{\mathrm{m}}(a/t)=1.12\sqrt{\pi\frac{a}{t}} \tag{9}$$

$$f_{\mathrm{b}}(a/t)=1.12\sqrt{\pi\frac{a}{t}}(1-\frac{4(a/t)}{\pi}) \tag{10}$$

where M_{kn} is the stress intensity amplification factor coefficient at the weld toe; a is the crack depth; n is the short crack extension index, and generally its value is 2; m is the long crack extension index, and generally, its value is 3.6; C is the crack growth constant; $I(r)$ is a dimensionless function of bending ratio r. In the case of a=0, the specimens in this article are the load control mode and its formula is as follows:

$$I(r)^{\frac{1}{m}}=\frac{1.23-0.364r-0.17r^2}{1.007-0.306r-0.178r^2} \tag{11}$$

where r is the load bending ratio:

$$r=\frac{|\Delta\sigma_{\mathrm{b}}|}{|\Delta\sigma_{\mathrm{s}}|} \tag{12}$$

The expression of equivalent structural stress is:

$$\Delta S_{\mathrm{s}}=\frac{\Delta\sigma_{\mathrm{s}}}{t^{\frac{2-m}{2m}}I(r)^{-\frac{1}{m}}} \tag{13}$$

The calculation formula of fatigue life after data fitting is:

$$N=(\Delta S_{\mathrm{s}}/C_{\mathrm{d}})^{-1/h} \tag{14}$$

Relevant parameters are shown in Table 5[19]:

Table 5 Main *S-N* curve parameters

Statistical basis	C_{d}	h
Mean	3 495.13	
+2σ	5 273.48	
−2σ	2 316.48	−0.277 12
+3σ	6 477.6	
−3σ	1 885.87	

4.3.2 Structural stress solution and life prediction based on finite element method

The fatigue life can be calculated by using Eqs.(3-14) and combining it with the node force nephogram in the two-dimensional model analysis. The finite element model needs to be re-established in this section. Commercial software Abaqus can be directly used to establish a three-dimensional model to calculate the node force of the welding position. Therefore, it is necessary to define the welding area elements, reference normal, weld initial node and initial element in advance when establishing the model. The model details are shown in Fig.14, and C3D8R solid elements were used for analysis. The number of meshes can be reduced because the equivalent structural stress method is not sensitive to mesh generation[20].

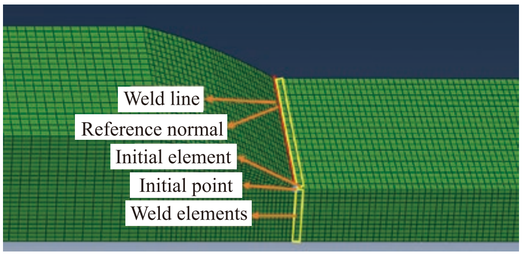

Fig.14 Definition of relevant parameters for calculating structural stress

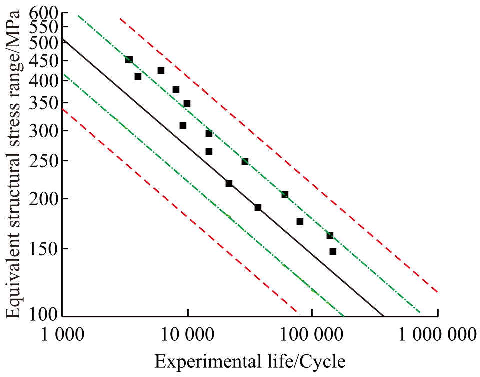

Fig.15 Experimental data and principal *S-N* curve of aluminum alloy

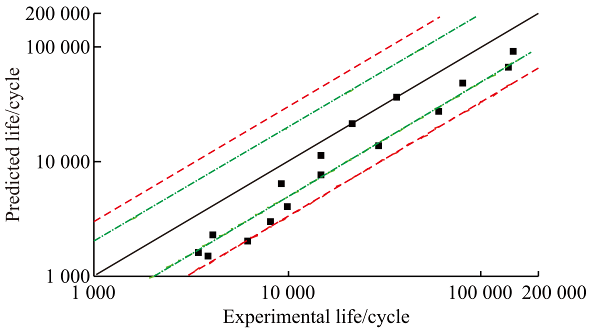

Fig.16 Life prediction results of equivalent structural stress method

The structural stress calculation results according to Eq.(13) were summarized in Table 6. The equivalent structural stress range was correlated with the experimental life in a double logarithmic coordinate system. The main *S-N* curves of $\pm 2\sigma$ and $\pm 3\sigma$ were drawn in Fig.15 with Eq.(14). It can be seen from Fig.15 that the fatigue test data have a good linear correlation. Most data are close to the curve of $+2\sigma$. Here, the curves described by $\pm 2\sigma$ represent approximately 95% prediction intervals, which is put forward in engineering applications in consideration of safety.

Table 6 Stress calculation results

Number	Structural stress range /MPa	Equivalent structural stress range /MPa
W01	401.464	409.319 12
W08	344.112	350.844 96
W05	286.76	292.370 8
W06	258.084	263.133 72
W09	372.788	380.082 04
W10	200.732	204.659 56
W12	215.07	219.278 1
Y01	172.056	175.422 48
Y02	243.746	248.515 18
Y03	143.38	146.185 4
Y04	415.802	423.937 66
Y07	444.478	453.174 74
Y08	451.647	460.484 01
Y09	157.718	160.803 94
Y11	301.098	306.989 34
Y13	186.394	190.041 02

The predicted fatigue life can be calculated by using Eq.(14) in Table 5. The results of fatigue life prediction based on the equivalent structural stress method are shown in Fig.16. The center line represents that the predicted life is equal to the experimental life. It can be seen from the figure that the predicted results are reasonable. Here the predicted lives are shorter than the experimental lives and the predicted results tend to be conservative. However, there is prediction data between the lower two-factor and the lower three-factor lines in the case of high stress and the prediction accuracy becomes conservative.

5 Discussion

The tensile strength of the welded joint is 188 MPa. The fatigue strength of 6061/7075 dissimilar aluminum alloy TIG welded joint can be calculated as 24.934 MPa according to the *S-N* curve fitted by Eq.(1). This is far lower than the tensile strength of both base metals and the welded joints. The experimental *S-N* curve presents a good linear relationship, which suggests that the welding quality is relatively stable although the tensile strength is low. The specimens with fractures near the welds on both sides have obvious deformation, and the fatigue life decreases significantly. This was not taken into account in the above subsequent analysis. The correlativity study showed that TIG welding of dissimilar aluminum alloys would produce defects such as pores and non-fusion. Cracks would initiate from the inside of the weld under the interaction of fatigue loads[21,22]. Incomplete fusion defects are more likely to cause a rapid decline in fatigue performance. It can be inferred that similar defects occur inside the weld of the partial specimens in this article.

Mehdi[23] conducted an XRD analysis on the TIG weld of 6061/7075 dissimilar aluminum alloy. A small amount of Al_2CuMg, $MgZn_2$, Al, and other intermetallic compounds was produced in the weld under the condition of ER5356 welding wire. These structures at the weld were also not considered in the above finite element stress analysis in order to simplify the model. At the same time, the notched stress method does not consider the residual stress after welding and other parameters, which will also affect the fatigue life. But the equivalent structural stress method can better reflect the real situation by synthesizing a principal *S-N* curve based on a large number of fatigue data, which includes the residual stress effect and the influence of various welding methods.

Weld reinforcement can have a significant impact on fatigue life, as it changes the degree of stress concentration at the weld toe. But it is difficult to measure in the finite element model, while its profile may be irregular. There may still be slight differences in different specimens under the same welding process. It is also overlooked in the previous analysis. How to associate weld reinforcement with predicting fatigue life is an important issue.

The notch stress method used in this paper can give a better prediction for the fatigue life of the specimens, and the prediction data are conservative and relatively accurate. The equivalent structural stress method comprehensively considers the influence of welded joint form, load boundary conditions, residual stress, and other factors on fatigue life. The characteristics of insensitivity to the mesh size make the finite element analysis more simplified. A main *S-N* curve can be used to quickly evaluate the fatigue life of the specimen. The finite element method combining with this curve can be more easily applied to the prediction of fatigue life. The prediction accuracy of the notch stress method decreases under low stress, while that of the equivalent structural stress method decreases under high stress, which can realize complementarity.

6 Conclusions

a) The final fatigue failure of 6061/7075 aluminum alloy TIG welding is mainly caused by 7075 side weld toe fracture. Although the tensile strength of 7075 base metal is higher, its fatigue strength is lower. The fatigue crack initiates from the toe and then extends along the thickness of the plate. The crack on the 6061 side has the risk of extending from the weld toe to the weld.

b) It is found that the weld area on the 7075 sides has a serious softening phenomenon, and the hardness has a serious sudden change when using ER5356 welding wire. However, the hardness of the 6061 side is relatively constant, and there is no obvious softening phenomenon with the 6061 side. The hardness value of the base metal area on both sides fluctuates greatly and the welding heat effect is serious.

c) Analyses show that the weld reinforcement can seriously affect fatigue life. The impact is greater under low stress, and fatigue life will decrease exponentially as the weld reinforcement increases. Weld reinforcement should be removed in practical applications.

d) This study finds that the errors of prediction results of the notch stress method are within two-factor lines, while the equivalent structural stress method is within three-factor lines, and both methods tend to give conservative results. Overall, the notch stress method gives more accurate life prediction results. The accuracy of the equivalent structural stress method in predicting life will deteriorate under high stress conditions, while the accuracy of the notch stress method in predicting life will deteriorate under low stress conditions.

Conflict of interest

All authors declare that there are no competing interests.

References

[1] Wang J T, Chen J W, Zhang Y K, *et al*. Influence of Ultrasonic Impact Treatment on Stress Corrosion of 7075 Aluminum Alloy and Its Welded Joints[J]. *Eng. Fail. Anal.*, 2023, 144: 106 908

[2] Niu P L, Li W Y, Yang C G, *et al*. Low Cycle Fatigue Properties of Friction Stir Welded Dissimilar 2024-to-7075 Aluminum Alloy Joints[J]. *Mater. Sci. Eng.: A*, 2022, 832: 142 423

[3] Deng A L, Chen H, Zhang Y B, *et al*. Prediction of the Influence of Welding Metal Composition on Solidification Cracking of Laser Welded Aluminum Alloy[J]. *Mater. Today Commun.*, 2023, 35: 105 556

[4] Wang Y J, Chen M A, Wu C S. HF Pulse Effect on Microstructure and Properties of AC TIG Butt-welded Joint of 6061Al Alloy[J]. *J. Manuf. Process*, 2020, 56(part A): 878-886

[5] Kumar P, Arif A, Prasad A C V S, *et al*. Study of Welding Process Parameter in TIG Joining of Aluminum Aolly (6061)[J]. *Mater. Today: Proc.*, 2021, 47(13): 4 020-4 025

[6] Dwivedi U, Tiwari S, Mishra A, *et al*. Comparative Study of Weld Characteristics of Friction Stir Welded Joints on Aluminium 7075 with Autogenous TIG[J]. *Mater. Today: Proc.*, 2020, 22(Part 4): 2 532-2 538

[7] Zhu Q Y, Lu P M, Xiang Q Y. Fatigue Life Evaluation of Web Butt Welding Structure on Boom of Excavator by Hot Spot Stress Approach[J]. *Eng. Fail. Anal.*, 2020, 113(2): 104 547

[8] Ren D Q, Jiang Y, Hu X A, *et al*. Investigation of Tensile and High Cycle Fatigue Failure Behavior on a TIG Welded Titanium Alloy[J]. *Intermetallics*, 2021, 132: 107 115

[9] Wan Z D, Meng D Y, Zhao Y, *et al*. Improvement on the Tensile Properties of 2219-T8 Aluminum Alloy TIG Welding Joint with Weld Geometry Optimization[J]. *J. Manuf. Process*, 2021, 67: 275-285

[10] Zhao H, Li M J, Wang X D, *et al*. Intergranular Corrosion Effect on Fatigue Behavior of Dissimilar 6005A-5083 Aluminum Alloys Weld Joints[J]. *Mater. Corros.*, 2022, 73(9): 1 505-1 518

[11] Chen Y J, Xu P D, Liu C C, *et al*. Multiaxial Fatigue Behavior and Life Prediction of 7075-T651 Aluminum Alloy under Two-step Loading[J]. *Eng. Fract. Mech.*, 2020, 230: 107 007

[12] Rotella G. Effect of Surface Integrity Induced by Machining on High Cycle Fatigue Life of 7075-T6 Aluminum Alloy[J]. *J. Manuf. Process*, 2019, 41: 83-91

[13] Zhao X Y, Xie S Q, Zhang Y L, *et al*. Fatigue Reliability Analysis of Metro Bogie Frame Based on Effective Notch Stress Method[J]. *Eng. Fail. Anal.*, 2022, 131: 105 811

[14] Wang Q D, Wang L B, Ji B H, *et al*. Modified Effective Notch Stress Method for Fatigue Evaluation of Rib-deck Welds Integrating the Critical Distance Approach[J]. *J. Constr. Steel Res.*, 2022, 196: 107 373

[15] Wang R J, Mi P. Study on Fatigue Strength of FSW Joints of 5083 Aluminum Alloy with Kissing Bond Defect[J]. *J. Mech. Sci. Technol.*, 2020, 34(7): 2 761-2 766

[16] Sonsino C M. A Consideration of Allowable Equivalent Stresses for Fatigue Design of Welded Joints According to the Notch Stress Concept with the Reference Radii rref = 1.00 and 0.05 mm[J]. *Weld World*, 2009, 53(3-4): R64-R75

[17] Zhang L Y, Dong P S, Wang Y D, *et al*. A Coarse-mesh Hybrid Structural Stress Method for Fatigue Evaluation of Spot-Welded Structures[J]. *Int. J. Fatigue*, 2022, 164: 107 109

[18] Liu Y, Deng C Y, Gong B M, *et al*. Fatigue Limit Prediction of Notched Plates using the Zero-point Effective Notch Stress Method[J]. *Int. J. Fatigue*, 2021, 151: 106 392

[19] Dong P S, Hong J K, Osage D A, *et al*. Master *S-N* Curve Method for Fatigue Evaluation of Welded Components[J]. *Weld. Res. Counc. Bull.*, 2002, (474): 1-50

[20] Li J, Zhang Q H, Bao Y, *et al*. An Equivalent Structural Stress-based Fatigue Evaluation Framework for Rib-to-deck Welded Joints in Orthotropic Steel Deck[J]. *Eng. Struct.*, 2019, 196: 109 304

[21] Yürük A, Çevik B, Kahraman N. Analysis of Mechanical and Microstructural Properties of Gas Metal Arc Welded Dissimilar Aluminum Alloys (AA5754/AA6013)[J]. *Mater. Chem. Phys.*, 2021, 273(2-3): 125 117

[22] Hima Bindu A, Chaitanya B S K, Ajay K, *et al*. Investigation on Feasibility of Dissimilar Welding of AA2124 and AA7075 Aluminium Alloy Using Tungsten Inert Gas Welding[J]. *Mater. Today: Proc.*, 2020, 26(Part 2): 2 283-2 288

[23] Mehdi H, Mishra R S. Effect of Friction Stir Processing on Mechanical Properties and Heat Transfer of TIG Welded Joint of AA6061 and AA7075[J]. *Def. Technol.*, 2021, 17(3): 715-727